

Design of Optimal LLCL Filter with an Improved Control Strategy for Single Phase Grid Connected PV Inverter

K. Arulkumar¹, D. Vijayakumar², K. Palanisamy³

¹Department of Electrical and Electronics Engineering, Madanapalle Institute of Technology and Science, Madanapalle, India

^{2,3}School of Electrical Engineering, VIT University, Vellore, India

Article Info

Article history:

Received Jul 12, 2017

Revised Jan 10, 2018

Accepted Jan 15, 2018

Keyword:

Damping loss

Feedback linearization

Grid PV inverter

LLCL Filter

ABSTRACT

The third order LLCL filter is gaining more attractive in grid connected PV inverter in terms of material cost saving than LCL filter. Several active and passive damping techniques prevail in mitigating the resonance problem for maintaining the grid power quality standards. In this paper an improved passive damping is examined with reduction of power loss for the LLCL filter. Particularly, it reduces the switching ripple much better than LCL filter, with a decrease in volume of the inductance. The filter design is also developed for the operation of stiff grid. Mathematical operations and transfer function are derived with frequency response for the accuracy of the filter design. In addition, comparative analysis of passive and improved passive damping control is proposed. The control strategy is improved with feedback linearization in order to avoid the glitches in inverter control and is verified with prototype grid connected PV inverter.

Copyright © 2018 Institute of Advanced Engineering and Science.

All rights reserved.

Corresponding Author:

K.Arulkumar,
Departement of Electrical and Electronics Engineering,
Madanapalle Institute of technology and science,
Madanapalle, 517 325, Andhrapradesh, India
Email: karuleee@gmail.com

1. INTRODUCTION

With the increase in distributed power generation systems (DPGs) it has become mandatory to supply excess power to the existing grid with the standard grid codes [1]. Figure 1. shows the generic structure of single phase grid connected PV inverter with controlled LCL filter design. The interconnection between DC converter and inverter is operated by dc-link capacitor.

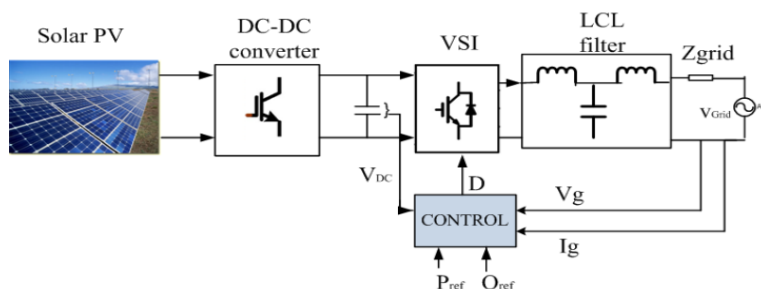


Figure 1. Control structure of single phase grid connected PV inverter

The power from the photovoltaic (PV) is injected into the grid through the voltage source inverter (VSI). Among many topologies [2]-[4], transformerless inverters have attracted due to its physical size with less space requirements and feasible cost constraints. The pulse width modulation (PWM) control is achieved by closed loop current control with the current harmonics less than 5% [5]. The switching frequencies between 2-15 kHz causes higher order harmonic disturbances in grid and losses. Higher order harmonics into the grid due to switching frequencies, leakage current and the electromagnetic interference (EMI) [6] noise are the significant issues in designing of filter circuit in the PV inverter.

Ripples and harmonics in the grid current can be reduced by filters connected at the output of the inverter [7]. The first order filter consists of one inductor connected in series known as L-filter which is most commonly used [8]. It does not have a resonance problem as compared to higher order filters. The inductor achieves reasonable attenuation of the current harmonics. The attenuation of 20 dB/decade is achieved for high frequency PWM converters. Higher order filters, LC & LCL have the combinations of inductors and capacitors, can give better attenuation of the harmonics with the disadvantages of complex design, cost and bulky [9]. The LC filter has better damping characteristics, but suffers from problem of infinite gain at resonance. In grid connected system, the resonance frequency of the filter varies with the inductance value of the grid [10]. The control of LCL filter is difficult compared to L filter, due to the presence of two more poles and zeros. Care must be taken to design a controller for additional poles and zeros that can make the system unstable if proper damping is not introduced. Damping of the LCL filter resonance can be either active using the converter, or passive using elements like resistors, capacitors and inductors. Several methods of passive damping [11]-[12] have been proposed for stiff grid operation. On the other hand, the active damping method is used with costly sensors and power electronics for weak grid and dynamic grid variations.

This paper mainly focuses on control structure of single phase grid connected PV inverter with filter design analysis. Section II illustrates the constraints of the LCL filter design and importance of Q-factor with sensitivity analysis. An improved LLCL filter is introduced, in order to reduce the total inductance of the conventional filter. The modified LLCL filter is designed without any change in the frequency response characteristic of LCL filter. More advantage in suppressing the resonance peak with improved stability and dynamic response. Three cases of parameter design have been differentiated and analyzed with simulated results in section III. Improved current control structure is seen in section IV by implementing feedback linearization for fast DC voltage control applied to PWM inverter. And it is verified by modeling a single phase grid connected PV inverter with simulated and experimental results.

2. SYSTEM DESCRIPTION AND CHARACTERISTICS

2.1. Classical Methods and Constraints on LCL Filter Design

In grid power converters, switching frequencies at intervals 3-20 kHz causes greater harmonics and disturbs the electric grid. It is therefore essential to attenuate the switching frequency harmonics and reduce the current ripples to fulfill the standards of the IEEE 1547.2. High frequency component currents would lead to electromagnetic interference noise mainly due to the parasitic capacitance disturbing the behavior of high frequencies. The method of designing LCL filters depends on rating of power converters, fundamental and switching frequency as inputs with an integrated control design of filters as explained in [13]. From the Figure 2 (a), the inverter output inductor L_1 , the filter capacitor C_f , and the grid-side inductor L_2 constitute the LCL filter of the inverter. Compared to L filter, LCL filter is proved to have a better harmonic attenuation for the reduction of filter inductance volume [14] which bypass the high frequency harmonics through the capacitance branch. The scope is to lower the higher order harmonics on the grid side and to reduce the oscillation effects. Therefore, in LCL filter design, inductors should be properly designed in observing the current ripple, filter capacitance and damping of resonance in filters. The resonant frequency should be in the range $10\omega_0 \leq \omega_{res} \leq \frac{\omega_{sw}}{2}$ [15]. Figure 2 (b), (c) depicts the passive damped topology of LCL filter. Frequency response analysis of passive damped LCL filters with damping resistors in series to attenuate the resonance with the transfer function as in (1) and improved methods with passive elements as in (2) are shown in Figure 3.

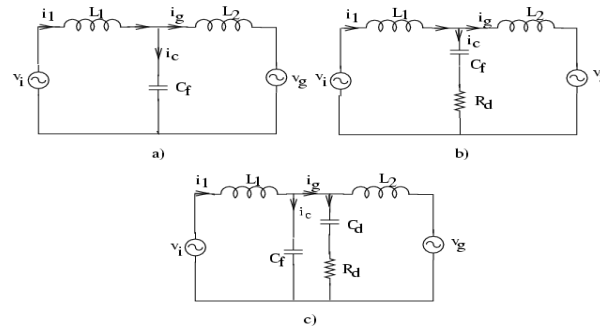


Figure 2. a). LCL filter, b) passive damped LCL filter with R_d , c) passive damped LCL filter with R_d - C_d

Transfer function of LCL filter:

$$G_{v_i \rightarrow i_g}(s) = \frac{i_g(s)}{v_i(s)} = \frac{1}{L_2} \frac{(S^2 + R_d C_f Z_{LC}^2 S + Z_{LC}^2)}{(S^2 + R_d C_f \omega_{res}^2 S + \omega_{res}^2)} \quad (1)$$

If R_d is zero then,

$$G_{v_i \rightarrow i_g}(s) = \frac{i_g(s)}{v_i(s)} = \frac{1}{L_2} \frac{(S^2 + Z_{LC}^2)}{(S^2 + \omega_{res}^2)}$$

Where,

$$Z_{LC}^2 = [L_1 C_f]^{-1}$$

$$\omega_{res}^2 = \frac{L_2 Z_{LC}^2}{L}$$

For improved passive damping,

$$G_{v_i \rightarrow i_g}(s) = \frac{i_g(s)}{v_i(s)} = \frac{(R_d C_d S + 1)}{S(L_1 L_2 R_d C_d C_f S^3 + L_1 L_2 (C_d + C_f) S^2 + R_d C_d (L_1 + L_2) S + L_1 L_2)} \quad (2)$$

From Figure 3 it is clear that the magnitude of LCL filter is high with a resonant peak gain of 250 dB at 4.6 kHz. However, in passive damping and improved passive damping, the attenuation is reduced to 10 dB or less than that at 2.5 kHz with some power loss due to the resistor.

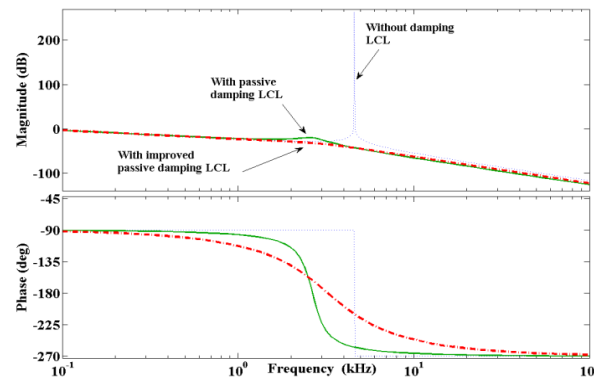


Figure 3. Frequency response of LCL filter

2.2. Selection of Filter Capacitance (C_f)

The selection of capacitor [16] is determined between reactive power in C_f and L_1 . If the capacitance is high, the reactive power flowing into it is more which leads to current demands in L_1 . In the design consideration large inductance (L_1) and smaller capacitance (C_f) lead to the voltage drop across the inductor L_1 . So, reactive power is chosen 15% of rated power as in (3) and from that the capacitance value can be chosen as:

$$C = 15\% \frac{P_{rated}}{3 \cdot 2\pi f_{line} V_{rated}^2} \quad (3)$$

Where, P_{rated} is rated power and V_{rated} is grid RMS voltage.

2.3. Significance of Q-factor Analysis

The importance of damping is to lower the Q-factor at the resonant frequency without affecting the frequency response at other frequencies. In Figure 3 frequency response analysis of higher order filter with and without damping is analyzed. The series LC circuit gives a minimum impedance at resonance while parallel LC circuit gives a maximum impedance at the resonant frequency. The value of Q-factor reduces in passive damping at a dominant resonant frequency [17]. The quality factor of L_f - C_f can be expressed as,

$$Q = \frac{1}{R_f} \sqrt{\frac{L_f}{C_f}} \quad (4)$$

For reducing the peak resonant, damping resistor is designed with an optimal Q-factor for the stiff grid condition. Increase of grid inductance can reduce the passive damping effect and cannot achieve the optimal Q-factor. Concurrently, the total power dissipation in the damping circuit is also an important parameter.

3. DESIGN OF MODIFIED LLCL FILTER

Based on the traditional LCL filter, a small inductor is inserted in the branch loop of the capacitor, composing a series resonant circuit at the switching frequency. It can, particularly, attenuate the switching-frequency current ripple components much better than the LCL filter, saves the total inductance and thereby leads to size reduction. The most convenient passive method is by adding physical resistors connected either in series or in parallel with inductor or capacitor of the filter. It aims at reducing Q-factor at dominant resonant frequency. Recently to reduce the inductor size a novel higher order LLCL filter [18] is proposed as shown in Figure 4 with transfer function as in (5)

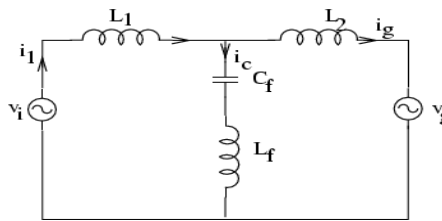


Figure 4. Schematic diagram of LLCL filter

Transfer function of $\frac{i_g(s)}{v_i(s)}$ LLCL filter is given as

$$G_{v_i \rightarrow i_g}(s) = \frac{i_g(s)}{v_i(s)} = \frac{L_f C_f s^2 + 1}{(L_1 L_2 C_f + (L_1 + L_2) L_f C_f s^3 + (L_1 + L_2) s)} \quad (5)$$

For LLCL, $\omega_{res} = \frac{1}{\sqrt{\left(\frac{L_1 L_2}{L_1 + L_2} + L_f\right) C_f}}$

3.1. Passive Damped Scheme of LLCL Filter

Modified LLCL filter topology [19] is used to reduce the damping power loss and high frequency harmonic attenuation as shown in Figure 5 (a), (b). Because of a series resonant circuit L_f - C_f is at switching frequency, the value of the inductor is much smaller than that of L_1 & L_2 . From the Figure 5 (b) passive damped LLCL₂ & Figure 2 (c) improved passive damped LCL, the value of damping parameters R_d and C_d is same. Most significantly, the total capacitance of (C_d+C_f) is encouraged to be less than 5% of apparent reactive power at rated load. From (6) and (7) it is to be noted that the addition of poles and zeros in a system gives rise to stability issues and care should be taken in designing the filters.

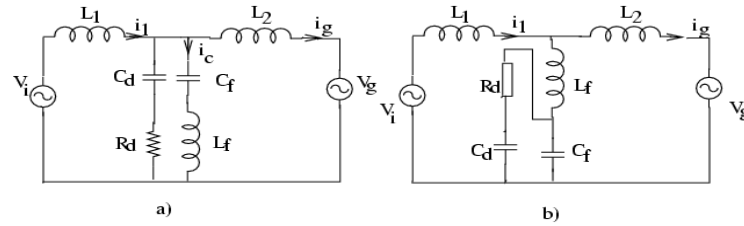


Figure 5. Various passive damped LLCL filters with R_d and C_d a). LLCL₁ b). LLCL₂

Bode plot of the transfer function of (1) & (5) is depicted as in Figure 6 a) and it is clear that an LLCL filter based grid connected VSI has almost same frequency response characteristic of LCL filter. In Figure 6 b) the peak magnitude lies within 20 kHz, the first resonant peak occurs at 7.6 kHz within half of the switching frequency and the next peak occurs at 20 kHz. The damping technique minimizes the resonant peak within the range. And it is worth mentioned that compared to LCL filter, the additional inductor L_f does not bring any control difficulties, an additional grid inductance L_2 is added to widen the bandwidth.

Transfer function of improved passive damping LLCL₁

$$G_{v_i \rightarrow i_g}(s) = \frac{i_g(s)}{v_i(s)} = \frac{s^3 A + s^2 B + s C + 1}{s^5 a + s^4 b + s^3 c + s^2 d + s e} \quad (6)$$

$$\begin{aligned} a &= L_1 L_2 L_f C_d ; \\ b &= ((L_1 L_2 + (L_1 + L_2) L_f) R_d C_d C_f) ; \\ c &= ((L_1 L_2 (C_d + C_f) + L_f C_f (L_1 + L_2)) ; \\ d &= R_d C_d (L_1 + L_2) ; \\ e &= (L_1 + L_2) ; \\ A &= L_f C_f C_d R_d ; \\ B &= L_f C_f ; \\ C &= R_d C_d ; \end{aligned}$$

Transfer function of improved passive damping LLCL₂:

$$G_{v_i \rightarrow i_g}(s) = \frac{i_g(s)}{v_i(s)} = \frac{s^3 A' + s^2 B' + s C' + 1}{s^4 b' + s^3 c' + s^2 d' + s e'} \quad (7)$$

$$\begin{aligned} b' &= ((L_1 L_2 + (L_1 + L_2) L_f) R_d C_d C_f) ; \\ c' &= ((L_1 L_2 (C_d + C_f) + L_f (C_f + C_d) (L_1 + L_2)) ; \\ d' &= R_d C_d (L_1 + L_2) ; \\ e' &= (L_1 + L_2) ; \\ A' &= L_f C_f C_d R_d ; \\ B' &= L_f C_f ; \\ C' &= R_d C_d ; \end{aligned}$$

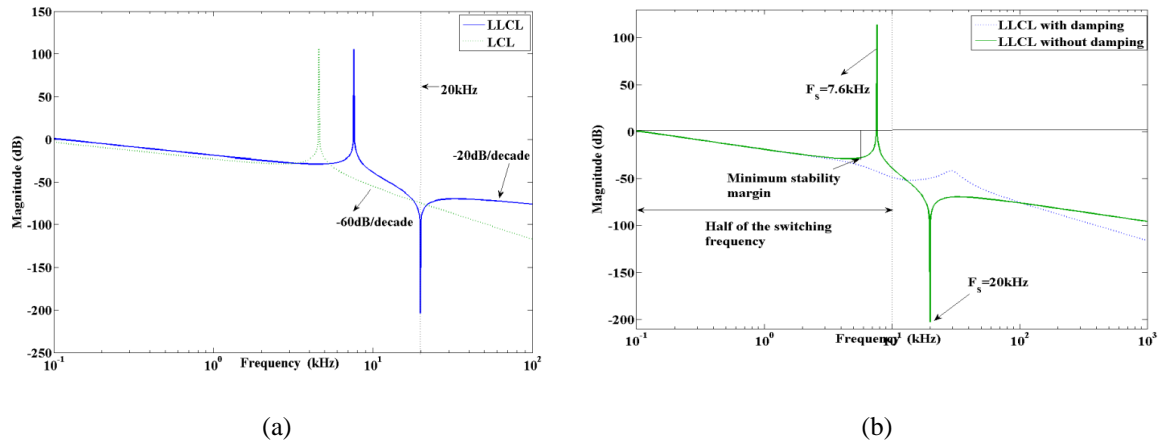


Figure 6. a).Frequency response analysis of LCL and LLCL, b). Frequency response analysis of damping techniques of LCL and LLCL

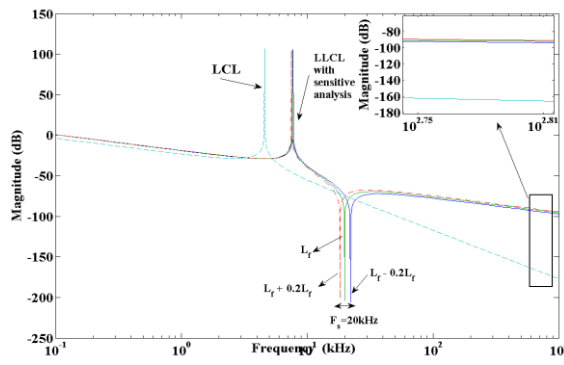


Figure 7. Sensitivity analysis of parameter variation of L_f ($\pm 20\%$)

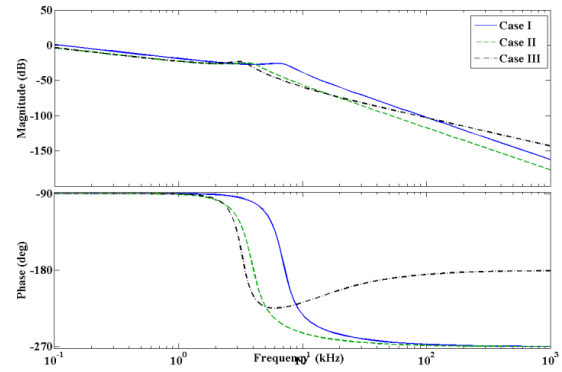


Figure 8. Frequency response analysis of passive damped LLCL

The bode plot of LCL and LLCL filter parameters, as given in Table 1 is plotted in Figure 7 with the sensitivity analysis on parameter variation of $\pm 20\%$. The enlarge view of magnitude of LLCL filter is also shown. Moreover, case I & case III as in Table 1 attenuate the resonance by -40 dB/decade, but in case II it is -60 dB/decade as in Figure 8. The designed LLCL filter attenuates resonant harmonics around the switching frequency and well suited for the single phase system.

Table 1. Filter Parameters in Design

Parameters	Case-I R_d damped LCL	Case-II $R_d - C_d$ damped LCL	Case-III $R_d - C_d$ damped LLCL
L1	1.2mH	1.2mH	1.2mH
R1	0.1 Ω	0.1 Ω	0.1 Ω
L2	1.2mH	1.2mH	0.22mH
R2	0.04 Ω	0.04 Ω	0.01 Ω
L_f	-	-	32 μ H
R_f	-	-	0.2 Ω
C_f	-	2 μ F	2 μ F
R_d	4 Ω	30 Ω	16.5 Ω
C_d	4 μ F	2 μ F	2 μ F

4. SYSTEM MODELING AND CONTROL STRUCTURE

Design of Optimal LLCL Filter with an Improved Control Strategy for Single Phase Grid ... (K. Arulkumar)

4.1. Proposed Inverter Current Control Strategy

The current injected into the grid by a power converter should keep a certain relationship with voltage at a point of connection. In order to avoid the glitches in the control of inverter it should be made more robust with the accurate parameter analysis. The block diagram in Figure 9 shows conventional current control loop structure [19] with grid side current feedback control. Where, $G_p(s)$ expressed as process gain & $G_c(s)$ denotes proportional resonant (PR) and harmonic compensator (HC) controller gain, $H(s)$ implies feedback gain of grid injected current, $G_{inv}(s)$ indicates gain of inverter and $G_{v_i \rightarrow i_g}(s)$ denotes a transfer function of LLCL filter, given by (5).

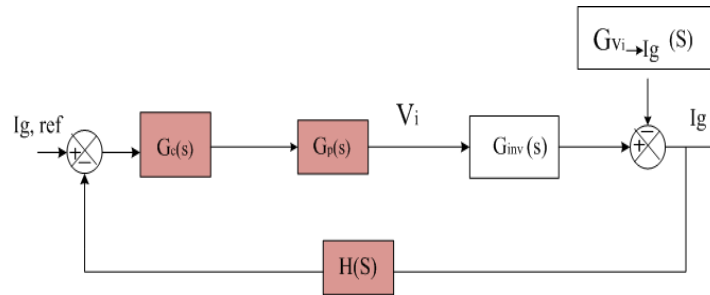


Figure 9. Inverter power control loop

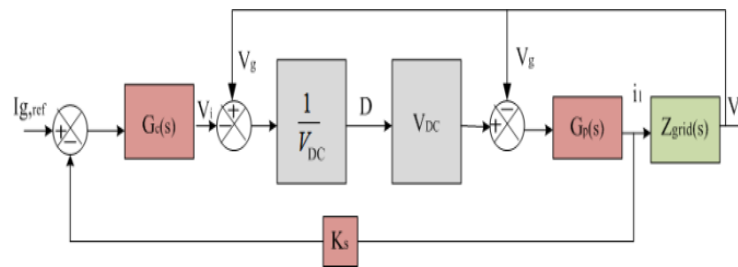


Figure 10. Proposed inverter current control structure

Table 2. Comparison on Different Cases

Parameters		CASE I LCL (R_d damped)	CASE II LCL (R_d - C_d damped)	CASE III LLCL
THD	Simulation	2.48 %	3.5 %	2.4 %
	Experimental	3.82 %	4.04 %	3.5 %
Damping Losses (W)	Calculated	2.51	0.89	0.45
	Measured	2.57	0.91	0.52

By considering the LLCL filter as shown in Figure 4, i_1 is the inverter current and the current flows through the capacitor i_c is being negligible compared to i_1 . The inverter current control structure as in Figure 10 exhibits the calculation of inverter current i_1 from the duty ratio (D) needs grid voltage (V_g) that is related to i_1 by the undetermined grid impedance (Z_{grid}). To avoid this problem, a nonlinear control technique from modern control theory named feedback linearization scheme [20], [21] is proposed. To exhibit the undetermined grid impedance, V_g is treated as a DC parameter. Compared to inverter current i_1 that is, the current loop crossover frequency is much higher than grid frequency. The Figure 10 also shows duty cycle (D) calculation from V_i using V_g and V_{DC} as defined in (8). With the proposed control the respective parameter makes the linear system with reduction in capacitor ripple current [22] and therefore reducing the size of the capacitor. The instantaneous current reference is used by the current compensator with the feedback current to provide a duty ratio to the inverter. The DC bus voltage is fixed at the desired set point and controlled current is injected into the grid. Here V_i controls the main inductor current I_L . The inverter current fed into the grid is given by (9). Where K_s represents the current feedback gain. Hence, the loop gain transfer function is expressed as,

$$G_{loop}(s) = G_c(s)K_sG_p$$

For the synchronization purpose, second order generalised integrator phase locked loop (SOGI-PLL) technique [23,24] is used to synchronize inverter voltage to the grid voltage and frequency.

$$D = \frac{(i_g^* - i_g) * G_c(s) + V_g}{V_{DC}} \quad (8)$$

$$i_g = \frac{(V_{DC} * D) - V_g}{Z_{LLCL}} \quad (9)$$

4.2. Experimental and Simulation Results

In order to verify the proposed damping technique and control structure, simulation is carried out using MATLAB/Simulink software. The parameters are the same as the designed in Table I. In order to verify the theoretical analysis, a 250 W experimental prototype as in Figure 11 based on a DSP (TMS320F28035) controller is constructed. A programmable DC power supply (chroma 62012P-80-60) is used to emulate the renewable energy sources. The grid current is sensed by current sensor ACS712ELCTR-20A, the type of IGBTs is IRFB4227PBF with switching frequency (F_s) as 20 kHz. A DC link capacitor of united chemi-con KXG series 450 V, 100 μ F is used. Total harmonic distortion (THD) is measured by the Fluke-434-Power quality analyzer and the waveform is obtained with agilent (MSO). Grid voltage and frequency are normally 230 V, 50 Hz.

With the feedback linearization control, Figure 12 shows the steady state experimental voltage response of dc-link voltage of 388 V as input to the inverter. The grid voltage and inverter output voltage synchronization in Figure 13 a) shows this as a promising current control structure with grid voltage and inverter voltage synchronized each other. The waveforms of inverter output voltage 388 V before filtering is shown in Figure 13 b). With the conventional LCL filter parameters the waveform of voltage and current is shown in Figure 14 with harmonics and spikes. To validate the proposed control structure and filter design, experimental results of both LCL and LLCL filter output waveform is compared in Figure 15.a), b). It shows that the proposed design of LLCL filter has less distortion in the waveform compared to LCL filter as the THD is 3.5 % with the proposed LLCL filter and 3.82 % with the conventional LCL filter as mentioned in Table 2. The results of the proposed grid connected system is shown in experimental results as in Figure 16 peak to peak voltage of 164.3 V and grid injected current of 2.2 A. The total harmonic distortion of the grid current in the laboratory is THD=3.5% as shown in Figure 17 that meets the IEEE 519 standard by measuring with the power quality analyzer FLUKE-434.

4.3. Result Analysis and Discussion

From the results it is to be that, increasing grid inductance can reduce the passive damping effect and increases the losses in the circuit in case I & II in Table I. However, in case III resonant peak occurs within the switching frequency with limited magnitude attenuation and current harmonic around it satisfy IEEE 519-1992. The current harmonic ($>=35^{th}$) is less than 0.3% of fundamental current by the parameter drift of L_f in range $\pm 20\%$ both in switching frequency and double of switching frequency. The proposed improved control strategy enhances the performances by introducing feedback linearization making linear structure in adding integrators to get fast and zero tracking errors and reducing the capacitor value as 100 μ F.

The total harmonic distortions of the grid side current in the three cases are measured using simulation and experiments and are listed in Table II. In case III, LLCL filter ($L_1=1.2$ mH, $L_2=0.22$ mH, $L_f=0.032$ mH) are used, of which the control performance of the grid inverter is shown in Figure 17 and THD is calculated as 2.4% in simulation and 3.5% in experimental. The damping loss calculation as in [8]. The power losses in the filter are mainly caused by inverter-side inductor current ripples of both LCL and LLCL filter. The damping power loss is mainly caused by volume of L_2 , L_f and R_d with the calculated and measured value of LLCL filter as 0.45 W and 0.52 W less than LCL filter.

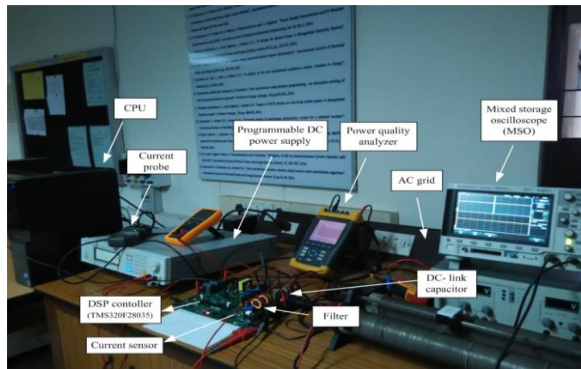


Figure 11. Laboratory setup of grid connected PV system

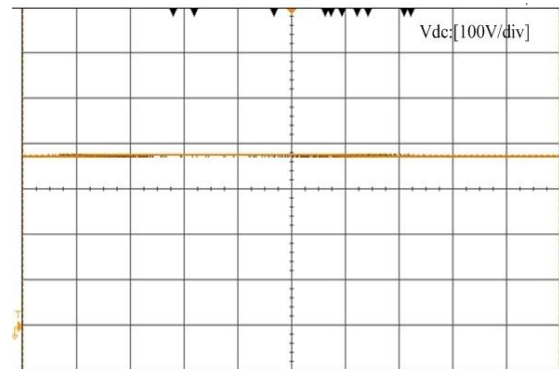
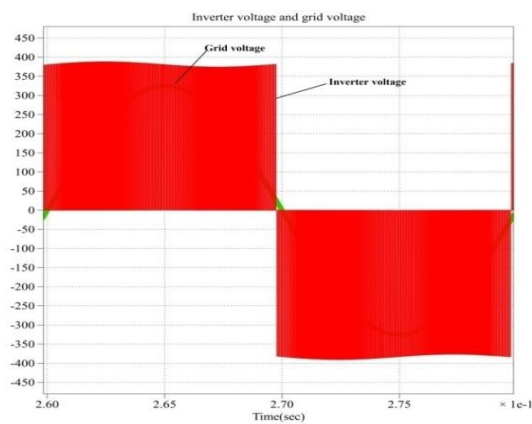
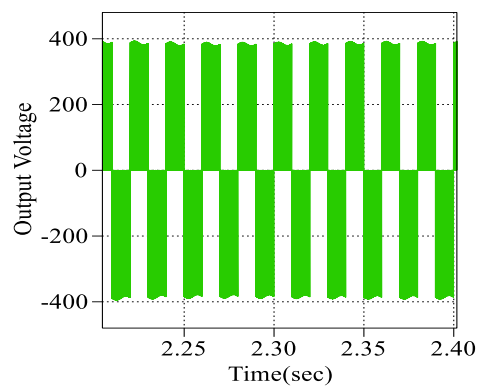


Figure 12. Experimental steady state DC bus voltage



(a)



(b)

Figure 13. (a) Synchronization of inverter voltage and grid voltage (b) Simulated inverter output voltage

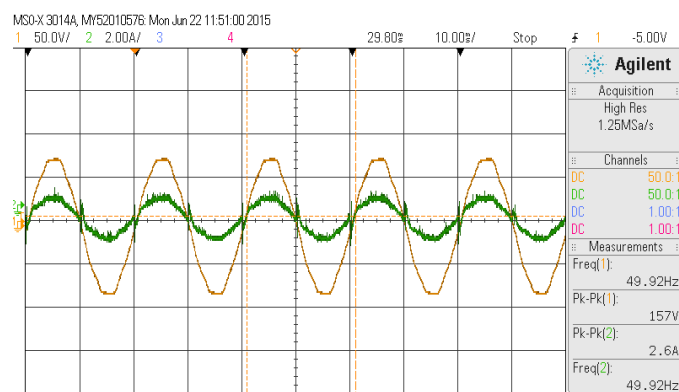


Figure 14. Experimental waveform of voltage and injected current into grid: a) with LCL filter

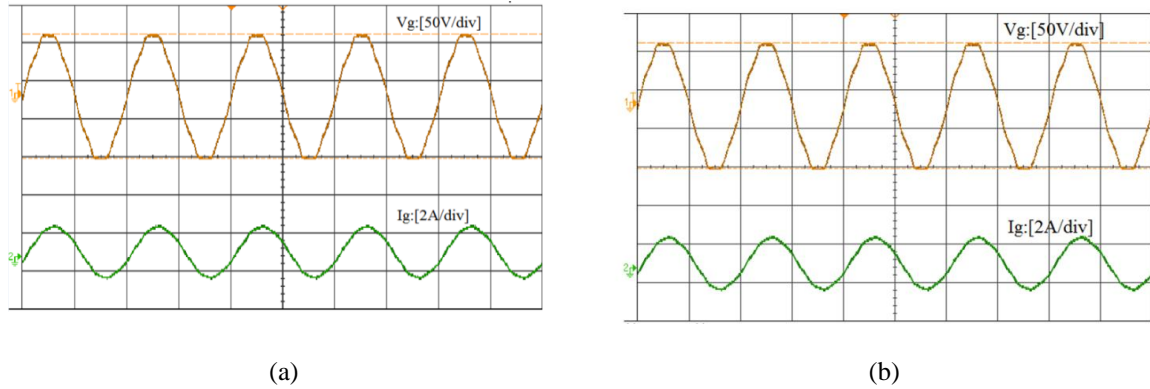


Figure 15. Experimental waveform of voltage and injected current into grid: a) with LCL filter as in case I and b) with LLCL filter as in case III

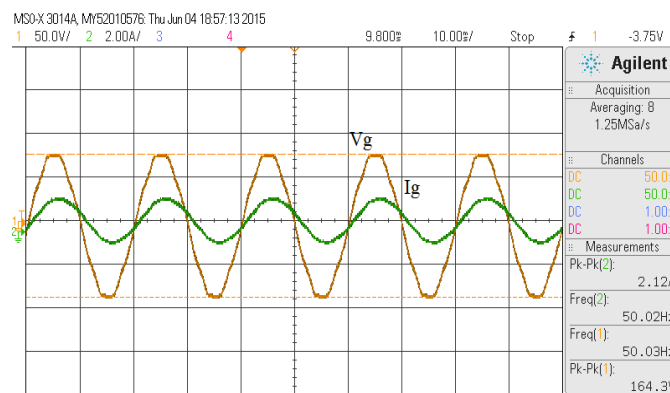


Figure 16. Experimental results of the proposed grid connected system

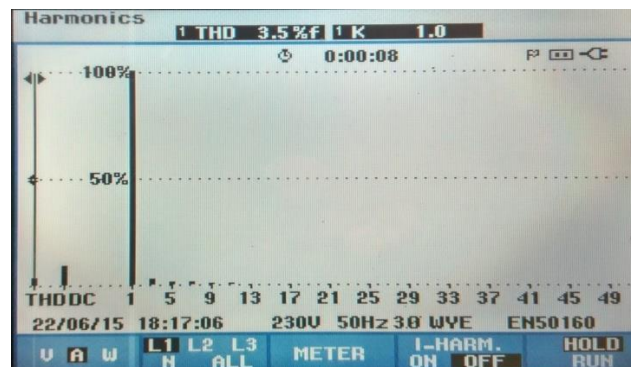


Figure 17. Snapshot of THD measurement

5. CONCLUSIONS

For reducing the resonance in the filter circuit, damping resistors are added with an additional inductance in LCL filter with improved control strategy is proposed in this paper. Comparative damping analysis of LCL and LLCL filter is designed with case parameters defined. Addition of passive elements and variation in filter parameters does not lose the stability. A Feedback linearization is used to control the duty ratio of inverter control for fast dynamic process, by adding integral control to eliminate steady state error that enhances the performance and shows satisfactory behaviour. The voltage transient is improved to decrease of current ripple and the size of the capacitor is reduced. The robustness of the system are verified using simulated and experimental results. The waveform of output current without any distortion shows that

the inverter with proposed control structure can convert solar power to a high quality power into the utility grid.

ACKNOWLEDGEMENTS

This work has been supported by power system research laboratory (TT-344), School of Electrical Engineering, VIT University, Vellore.

NOMENCLATURE

V_i	inverter voltage (V)	i_l	inverter current (A)
V_g	grid voltage (V)	i_g	grid current (A)
P_{rated}	rated power (W)	V_{rated}	rated voltage (V)
f_{grid}	grid frequency (Hz)	V_{DC}	dc bus voltage (V)
C_f	filter capacitance	R_d	damping resistor
C_d	damping capacitance	$\omega_{resonant}$	frequency
ω_0	fundamental frequency	Z_{grid}	grid impedance
D	duty ratio		

REFERENCES

- [1] IEEE Application Guide for IEEE Std. 1547 IEEE standard for interconnecting distributed resources with electric power systems, *IEEE 1547.2-2008*, 2009.
- [2] S. Kouro, Leon, J. I., Vinnikov, D., and Franquelo, L.G., Grid-connected photovoltaic systems: An overview of recent research and emerging PV converter technology, *IEEE Indus. Electron. Mag.*, vol.9(1), pp.47-61, 2015
- [3] Srikanth, S., A Three Phase Multi Level Converter for grid Connected PV System. *International Journal of Power Electronics and Drive Systems (IJPEDS)*, 5(1), pp.71-75, 2014.
- [4] B.N.Alajmi, Ahmed, K. H., Adam, G. P., and Williams, B. W., Single-phase single-stage transformer less grid-connected PV system, *IEEE Trans. Power Electron.*, Vol.28(6), pp. 2664-2676, 2013.
- [5] F. Blaabjerg, R. Teodorescu, M. Liserre, and A. Timbus, Overview of control and grid synchronization for distributed power generation systems, *IEEE Trans. Ind. Electron.*, 53(5) pp. 398-1409, 2006.
- [6] G. L. Skibinski, R. J. Kerkman, and D. Schlegel, EMI emissions of modern PWM AC driver, *IEEE Ind. Appl. Mag.*, 5(6), pp. 47-80, 1999.
- [7] Itoh, J-I., and Fumihiro Hayashi, Ripple current reduction of a fuel cell for a single-phase isolated converter using a DC active filter with a center tap, *IEEE Trans. Power Electron.*, 25(3), pp. 550-556, 2010.
- [8] K. Arulkumar, P. Manojbharath, S. Meikandasivam and D. Vijayakumar, "Robust control design of Grid power converters in improving power quality," 2015 International Conference on Technological Advancements in Power and Energy (TAP Energy), pp. 460-465, 2015.
- [9] W.Wu, Y. He, T. Tang, and F. Blaabjerg, A new design method for the passive damped LCL and LLCL filter-based single-phase grid-tied inverter, *IEEE Trans Indus Electron.*, 60(10), pp. 4339-4350, 2013.
- [10] Wu, Weimin, Yuanbin He, and Frede Blaabjerg. An LLCL power filter for single-phase grid-tied inverter, *IEEE Trans. Power Electron.*, 2(2) (2012) 782-789.
- [11] Zhao, Wenqiang, and Guozhu Chen, Comparison of active and passive damping methods for application in high power active power filter with LCL-filter, Proc. of IEEE SUPERGEN, 1-6, Apr. 2009.
- [12] M. Liserre, R. Teodorescu, and F. Blaabjerg, *Stability of grid-connected PV inverters with large grid impedance variation*, Proc. Of IEEE PESC, Aachen, Germany, pp. 4773-4779, Jun. 2004.
- [13] Z. Zeng, J.-Q. Yang, S.-L. Chen, and J. Huang, Co-design of the LCL filter and control for grid-connected inverters, *Journal of Power Electronics*, vol.14(4), pp.1-10, 2014.
- [14] Arulkumar, K., Manojbharath, P., Meikandasivam, S. and Vijayakumar, D., *Robust control design of Grid power converters in improving Power Quality*. IEEE International Conference, pp. 460-465, 2015.
- [15] M. C. Di Piazza, A. Ragusa, and G. Vitale, Design of grid-side electromagnetic interference filters in ac motor drives with motor-side common mode active compensation, *IEEE Trans. Electromagn. Compat.*, vol.51(3), pp.673-682, 2009.
- [16] Liserre, Marco, Frede Blaabjerg, and Steffan Hansen. Design and control of an LCL-filter-based three-phase active rectifier, *IEEE Trans. Ind. Appl.*, vol.4(5), pp.1281-1291, 2005.
- [17] Wu, Weimin, Yuanbin He, and Frede Blaabjerg, An LLCL power filter for single-phase grid-tied inverter, *IEEE Trans. Power Electron.*, vol.27(2), pp. 782-789, 2012.
- [18] P. Alemi, S.Y.Jeong, and D.C. Lee, Active Damping of LLCL Filters Using PR Control for Grid-Connected Three-Level T-Type Converters, *Journal of Power Electronics*, vol. 15(3), pp. 786-795, 2015.
- [19] Wu, W., Sun, Y., Huang, M., Wang, X., Wang, H., Blaabjerg, F., and Chung, H. S. H. A robust passive damping method for LLCL-filter-based grid-tied inverters to minimize the effect of grid harmonic voltages, *IEEE Trans. Power Electron.*, vol. 29(7), pp. 3279-3288, 2014.

- [20] G. Shen, Xu, D., Cao, L., and X. Zhu, An improved control strategy for grid-connected voltage source inverters with an LCL filter, *IEEE Trans. Power Electron.* Vol. 23(4), pp. 1899-1906, 2008.
- [21] D.C. Lee, G-Myoung Lee, and Ki-Do Lee, DC-bus voltage control of three-phase AC/DC PWM converters using feedback linearization, *IEEE Trans. Ind. Appl.*, vol. 36(3), pp.826-833, 2000.
- [22] A. J. Krener, Mathematical Control Theory, Springer, chap.3, pp.66-98, 1999.
- [23] D.E. Kim, and D.C. Lee, Feedback linearization control of grid-Interactive PWM converters with LCL filters, *Journal of Power Electronics*, Vol. 09(2), pp. 288-299, 2009.
- [24] K. Arulkumar, K. Vijayakumar, and K. Palanisamy. "Recent advances and control techniques in grid connected PV system—A review." *International Journal of Renewable Energy Research*, Vol.6 (3), pp.1037-1049, 2016.

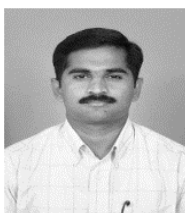
BIOGRAPHIES OF AUTHORS



K. Arulkumar was born in 1986. He received the B.E. degree in Electrical & Electronics from Anna University, Chennai, in april 2008 and M.Tech (Power Electronics) degree from VelTech Dr.RR & Dr.SR Technical University, Chennai in may 2011. He did in Ph.D in VIT University, Vellore, India. His research interest include Grid connected Inverter control & solar PV system integration.



D. Vijayakumar received his Bachelor Degree in Electrical and Electronics Engineering and Master Degree in Power Systems in the year 2002 and 2005 respectively. He received his Doctorate in April 2010 at Electrical Department in Maulana Azad National Institute of Technology (MANIT), Bhopal, India. Presently, He is an Associate Professor & Program Chair of EEE and Division Chair of Power Systems in the School of Electrical Engineering, VIT University, Vellore, India. His research interest include power system protection, and Renewable energy sources.



K. Palanisamy received his Bachelor degree from University of Madras, Chennai, India, and the M.E. degrees from Anna University, Chennai, India, Ph.D from VIT University Vellore, India in 2000, 2004 and 2013, respectively. In 2004, he joined the Department of Electrical & Electronics Engineering in Kongu Engineering College, Erode, as a Lecturer. Presently, he is an Associate Professor with the School of Electrical Engineering, Vellore Institute of Technology, Vellore, India. He is a certi_ed Energy Auditor by Bureau of Energy Ef_ciency, Government of India. His research interests are in power quality, energy conservation and renewable energy integration.